

# Using simplified meshes for crude registration of two partially overlapping range images

Mercedes Rocío Gonzales Márquez  
Computer Science Course  
State University of Matogrosso do Sul  
P.O.Box 351, 79804-970 – Dourados, MS, Brazil  
mercedes@uems.br

Wu, Shin - Ting  
School of Electrical and Computer Engineering (FEEC)  
State University of Campinas (Unicamp)  
P.O.Box 6101, 13083-970 – Campinas, SP, Brazil  
ting@dca.fee.unicamp.br

## ABSTRACT

We present an efficient algorithm for crude registration of two partially overlapping range images. The central focus of our work is how to filter out the wrong pairs efficiently in order to reduce the search space. Motivated by the availability of robust and efficient mesh simplification algorithms, such as the QSLIM software package, which preserve the main characteristics of the surface shape, we propose to find a good initial transformation estimate on the basis of the vertices of simplified meshes, instead of the original dense sets of range data. Promising results, that make the iterative closest point matching procedure converges to a correct final alignment, are provided.

**Keywords** Crude registration, Range Images.

## 1 INTRODUCTION

A range image is a two-dimensional grid of depth measurements of a sampling of surface points presented in a scene. As the depth of each imaged point in a given range image is measured from a plane or a single point on the range sensor that captured it, the coordinates of the acquired data are usually represented in terms of the position of this reference. Nevertheless, because of the three-dimensionality of most of objects of interest, this acquisition procedure cannot completely cover an object. Thus, for getting a 3D data model, the capture of several images acquired from different points of view is necessary, as illustrate Figures 1 and 2, and these images may need to be calibrated to a common (global) reference system in a process called *views alignment* or *registration*.



Figure 1: Range images of an angel.



Figure 2: Range images of a dragon.

The registration problem of two partially overlapping range images, *S*-image and *D*-image, may be splitted into two coupling problems: *correspondence* and *pose* [BMW05a]. A *correspondence* refers to find out the points or features from *S*- and *D*-images that are matchable, and the *pose* problem consists in determining the rigid transformation  $T$  (rotation  $R$  and translation  $t$ ) that may need to be applied on the range data to overlap the matchable points in a common reference system.

Mathematically, for finding the rigid transformation  $T$ , represented by a  $4 \times 4$  matrix, at least three matchable pairs  $(p_i, q_i)$  are required, being  $p_i$  samples of *S*-image and  $q_i$  samples of *D*-image. These pairs must satisfy the equation  $q_i = T p_i$ . If  $N$  pairs are known,  $N > 3$ , the registration problem is, usually, solved by the least squared method  $\min f$  where  $f = \frac{1}{N} \sum_{i=1}^N \|q_i - T p_i\|$ . However, the matchable points are, in most cases, not known. We must estimate them, evaluate the estimated matchable points on the basis of a *fitness error* criterion, and carry the process out iteratively, until a solution with a *fitness error* under the pre-specified tolerance is achieved. Figure 3 shows the registered images of the image pairs presented in Figures 1 and 2.

With respect to the initial estimate, we may classify the existing automatic registration algorithms into two

Permission to make digital or hard copies of all or part of this work for personal or classroom use is granted without fee provided that copies are not made or distributed for profit or commercial advantage and that copies bear this notice and the full citation on the first page. To copy otherwise, or to publish, to post on servers or to redistribute to lists, requires prior specific permission and/or a fee. Copyright UNION Agency – Science Press, Plzen, Czech Republic.

groups: a one-step and a two-step technique. A one-step method aims at obtaining a precise transformation *T en masse*, taking all potential matchable points into consideration. Thus, the problem is dealt with as a 6-dimensional optimization problem. Some researchers apply the genetic algorithm (GA) to find its global minimum, which is theoretically the best solution [KA96, CR02]. To overcome the low convergence of such algorithms, a hybrid genetic algorithm (HGA) that combines the GAs with a numerical method, such as the Quasi-Newton (hill climbing) one is proposed [RP96]. Silva et al. also adopt this approach to get an accurate registration [LK05]. Despite of several efforts, a one-step procedure is still computationally expansive.

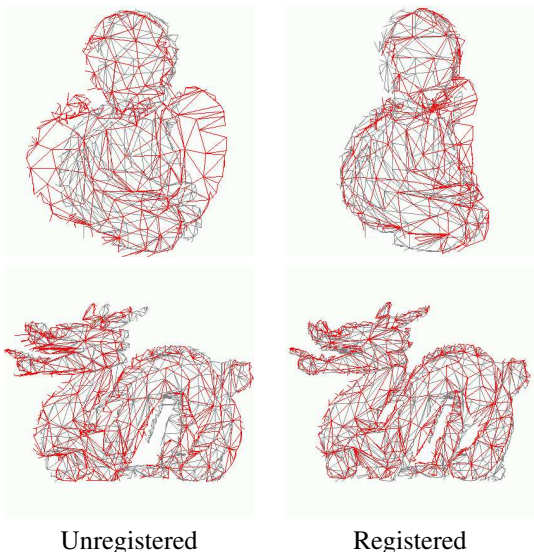


Figure 3: Crude registration of angel and dragon's images.

The basic idea underpinning a two-step method is to handle the problem in two stages: firstly the images are matched from their intrinsic features, then they are finely tuned in order to minimize the point-to-point distance, or the extrinsic, errors. These two steps are, respectively, called the crude registration and the fine registration. From numerical point-of-view, the crude registration, on the basis of the complete collection of samples, provides a good initial estimate  $T_0$  to the fine registration. This, in its turn, attempts to iteratively adjust the transformation matrix, in order to minimize the mean squared errors between the supposed correspondences. The iterative closest point (ICP) [BM92, CM92] and its variants are examples of this category of procedures [RL01].

While the ICP algorithm is recognized as an efficient algorithm for the second step, a robust technique for obtaining  $T_0$  is still pursued by the researchers [WG02, BMW05a]. As detailed in Section 2, the crude registration algorithms basically distinguish in the intrinsic geometric properties that they use for comparison

purposes and in the size of the data that they process for getting plausible local correspondences. If no landmarks are provided, it is still a challenging problem how to *automatically* and *efficiently* extract from the dense data sets the information that is effectively essential for correspondences.

In this paper, we propose to reduce the size of data sets by simplifying the *S*- and *D*-images into *S*- and *D*-meshes with much fewer triangles. Figure 1.(b) illustrates a simplified mesh of the original data set depicted in Figure 1.(a). Though the number of vertices is drastically reduced from 24540 to 200, the vicinity of all the vertices of the simplified mesh keeps the property to be locally alike. Hence, we conjecture that a simplified mesh that preserves the global geometric characteristic of the original data suffices for a coarse registration.

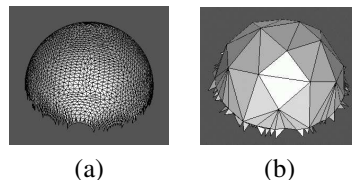


Figure 4: Simplification of a symmetric mesh.

Our proposal is founded on the fact that for crude registration only the geometrically distinguishing features of the input images are of interest. Hence, we may “blur” the local geometrical properties of the input image in such a way that only globally relevant geometric characteristics are kept. From the remaining samples we may get a transformation matrix  $T_0$  that can bring *S*- and *D*-images close enough and that can ensure the convergence of any ICP-like algorithm. We should, therefore, elaborate a mesh simplification algorithm that delivers faithful approximations, namely the *S*- and *D*-meshes, to these dense data.

The *S*- and *D*-meshes may contain distinct number of vertices and possess distinct topology. Comparison strategies, such as the spin-image and the geometric histogram matching, are not applicable in our case. In principle, we may adopt the random sample consensus based data aligned rigidity constrained exhaustive search schema. Nevertheless, after simplification, the size of our input data for registration becomes much smaller and we may exhaustively look for appropriate matchable structures in the *D*-mesh for each structure in the *S*-mesh. This increases the confidence of our search procedure.

Experimentally, we found that the mesh simplification procedure in the QSLIM software package [GP97] satisfies our simplification requirements. A brief description of the algorithm is given in Section 3. The remaining issue is how to construct faithful structure that lead us to a good estimate for  $T_0$ . In Section 4, we provide the geometric metrics that we use to automatically construct the matching structure in the *S*-mesh and

the procedure that we adopt to find a matchable one in the  $D$ -mesh, and consequently, the required alignment transformation. In Section 5 the results that validate our proposal are presented. Finally, in section 6 further work is discussed.

## 2 RELATED WORKS

The algorithms for crude registration work either on the basis of the geometric measurements of the whole sample points with regard to a small set of points, or on the basis of the geometrical characteristics of the vicinity of this small set of points. As far as we know, they work on the dense original range data.

In *Spin-image matching (SIM)* procedure, a small number of oriented points is randomly chosen from  $S$ -image [AM99]. From each of those points, a spin-image is generated, consisting of a 2D-histogram constructed by the radial distance (to the surface normal at the oriented point) and the axial distance (to the tangent plane at the point) of all other points. Then, spin-images associated to distinct points of the  $D$ -image are compared with a few set of the previously built spin-images for constructing matched pairs and estimating transformation candidates. False transformations are pruned by the ICP algorithm. According to the careful comparisons carried out by Planitz et al. [BMW05a], this technique may take a long time and require excessive storage for high resolution surfaces. Moreover, it may fail when the models are axis-symmetric [BMW05b]. Our proposed method not only has less storage complexity but is suitable for axis-symmetric models, as well. We will show that our procedure can successfully register a pair of the axis-symmetric hub's range data presented in Figure 5.

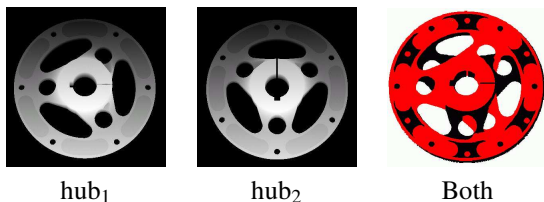


Figure 5: A pair of hub's range images

Instead of histograms constructed by the radial and the axial distances, *Geometric histogram matching (GHM)* method is based on a few set of histograms from the triangular mesh of the  $S$ -image, each of which represents the relative angle between the normal of a given facet  $f_i$  and all other surrounding facets, within a predefined distance from the plane in which  $f_i$  lies to all points of the surrounding facets [AFWR98]. A match for facet  $f_i$  is determined by finding the best match between its histograms and the histograms representing the facets of the triangular mesh of the  $D$ -image. The Random Sample Consensus (RANSAC) algorithm [MR81] is used to compute the best orientation and the best translation for a plausibly correct

final alignment. It was verified that GHM is unsuitable for surfaces with few distinct surface curvature variations [BMW05a]. In this work, we show that our proposed method also works well on models with smooth curvature variations, such as the pairs of images in Figures 6 and 7. In the both cases abrupt curvature transitions are concentrated in a very small region.

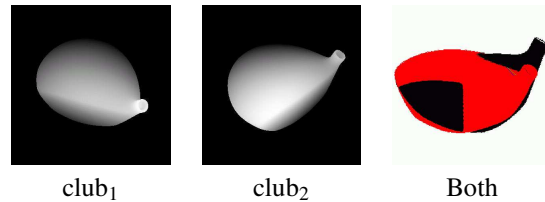


Figure 6: Ranges images of a club.

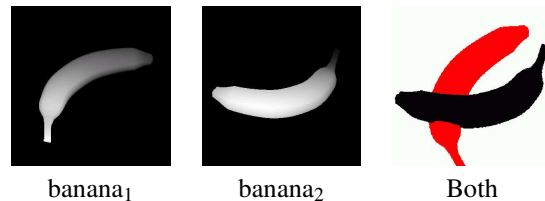


Figure 7: Ranges images of a banana.

*RANSAC-based DARCES (RBD)* is an acronym for Random Sample Consensus based Data Aligned Rigidity Constrained Exhaustive Search [CHC99]. Differently from the SIM and the GHM techniques, it does not require the computation of the geometrical characteristics of the whole sample points. In each iteration of the RBD algorithm, a sample point  $s_1$  is randomly chosen from  $S$ -image, which together with two nearby non-collinear sample points  $s_2$  and  $s_3$  builds a triangular structure  $L$ . Each sample in  $D$ -image is then exhaustively tested aiming to find a triangle that is matchable to  $L$ . For the first point  $s_1$ , any point of  $D$ -image is considered as a potentially matchable point  $m_1$ . The search region for the corresponding point  $m_2$  to  $s_2$  can be limited to the sphere of radius  $d_{12}$  centered at  $m_1$  where  $d_{12}$  is the distance between  $s_1$  and  $s_2$ . And the search region for the corresponding point  $m_3$  to  $s_3$  can be further limited to the intersection of two spheres, one centered at  $m_1$  with radius  $d_{13}$  and the other centered at  $m_2$  with radius  $d_{23}$ . For evaluating the quality of alignment transformation, the authors use a subsample of the original data. Although it works for a wide variety of surfaces, it may take a long time for finding a good initial estimate that converges to a correct alignment. Instead of a planar structure, we propose to use a spatial structure. Because a spatial structure is more distinguishable, fewer matchable structures are selected, which makes feasible to test all of them for getting the best one. Although the modified RBD algorithm implemented by Planitz et al. successfully matches the DINO surface pair presented

in Figure 8 [BMW05a], the outcome of our proposed algorithm is quantitatively and qualitatively better.

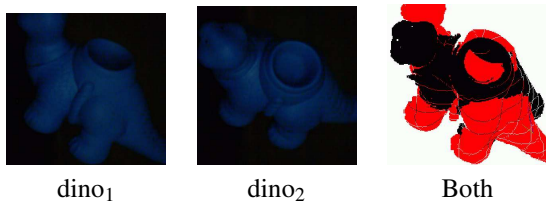


Figure 8: Ranges images of a dinosaur.

In the *Intrinsic curve matching (ICM)* procedure, curves with zero mean curvature are extracted from range images [KPH02]. For each individual range image, all possible pairings between curves are established. In each pairing, the shortest line segment (connector) is determined in *S*-image and its length is used for finding the best correspondence in *D*-image. The quality of the transformation is evaluated by the number of feature alignments. According to Planitz et al. [BMW05a], it works better on surfaces with smooth curvature variations than those with sharp edges. Thus, it fails to perform a good alignment for the pair of images of an object with hard edges, such as the images in Figure 9. Contrary to the ICM algorithm, our proposed model does not suffer from this restriction.

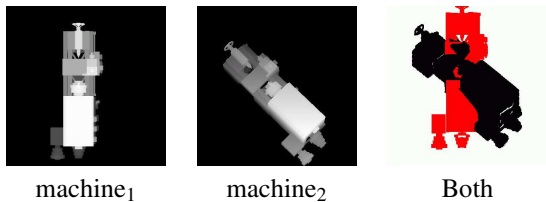


Figure 9: A pair of a machine's images.

### 3 DATA SIMPLIFICATION

To be self-contained, we provide a brief description of the efficient simplification algorithm implemented in the QSLIM package. It uses iterative edge contractions on the basis of quadric errors associated to each vertex  $v$ .

The squared distance of  $v$  to an adjacent face  $k$ , represented by  $n_k \cdot v = d$ , may be expressed as

$$\begin{aligned} D^2(v) &= (n_k^t v + d)^2 = (v^t + d)(n_k^t v + d) \\ &= v^t (n_k n_k^t) v + 2d n_k^t v + d^2 \end{aligned} \quad (1)$$

which may be written in a quadratic form

$$Q(v) = v^t A v + 2b^t v + c = D^2(v)$$

by making  $A = n_k n_k^t$ ,  $b = d n_k$ ,  $c = d^2$ .  $Q$  can be defined as a triple  $Q = (A, b, c)$  where  $A$  is a  $3 \times 3$  matrix,  $b$  is a 3-vector, and  $c$  is a scalar. The addition of quadrics is performed componentwise:  $Q_i(v) + Q_j(v) = (Q_i + Q_j)(v)$  where  $(Q_i + Q_j) = (A_i + A_j, b_i + b_j, c_i + c_j)$ . The

quadric error  $E$  associated to  $v$  is given in terms of the sum of squared distance to all its adjacent faces

$$E(v) = \sum_k D_k^2(v) = \sum_k Q_k(v) = Q(v).$$

Observe that the initial quadric error estimate for each vertex is 0, since it lies in the planes of all its adjacent faces.

Let  $e_{ij}$  be edges of a triangular mesh whose extreme vertices are  $v_i$  and  $v_j$  and  $Q_i$  and  $Q_j$  be their associated quadrics, respectively. In each iteration of the simplification algorithm, the optimal contraction  $\bar{v}$  for each edge is computed (Figure 10), such that the quadric error of its substitute  $\bar{v}$ ,  $Q(\bar{v}) = Q_i(\bar{v}) + Q_j(\bar{v})$  has the minimal quadric error. Since  $Q(\bar{v})$  is quadratic, finding its minimum is a linear problem. The minimum occurs where  $\partial Q / \partial x = \partial Q / \partial y = \partial Q / \partial z = 0$

$$\Delta Q(v) = 2Av + 2b = 0$$

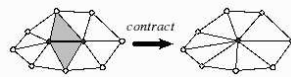


Figure 10: Edge contraction

Assuming that  $A$  is invertible, one gets  $\bar{v} = -A^{-1}b$ . Among all the computed quadric errors, the edge that presents the lowest quadric error is selected to be contracted and the quadric errors of the adjacent vertices are updated. The process is repeated, until the desired level of simplification is reached.

This simplification process satisfies our filtering requirement, which is to “blur” the geometric properties, or to cluster the samples into a vertex, such that the global prominent shapes are preserved, that is, a quadric error of the substitute is less than the specified tolerance.

Figure 3 presents the simplified mesh of a face with several prominent shapes. Observe that, even with a reduced number of vertices, from 3717 to 200, we may still distinguish the nose, eye, chin, cheek, and the hair's comb.

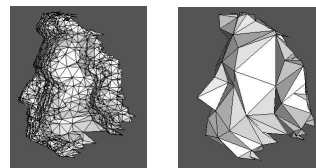


Figure 11: Simplification of a mesh with prominent features.

### 4 CRUDE REGISTRATION

Using a pair of simplified meshes to determine a possible alignment transformation reduces the search space for potential correspondences. Hence, it is expected

that the efficiency of the process is improved. Now, it remains to show how to derive the transformation matrix  $T_0$  from the two simplified meshes. We may adopt either a global optimization method, that takes into consideration the complete collection of vertices of the simplified meshes and involves the solution of a larger system of equations, or a locally aware approach by defining spatial structures with fewer vertices in the  $S$ -mesh and looking exhaustively its pair in the  $D$ -mesh. Aiming at efficiency and robustness, we present in this section a solution for the second approach. The basic idea is to explore the sparsity of the simplified meshes and perform a computationally efficient global search among all of their vertices.

#### 4.1 Defining Matching Structures

Once any isometric transformation in  $\mathfrak{R}^3$  may be characterized by three linearly independent vectors, we propose to use a spatial structure for pairing the vertices of  $S$ - and  $D$ -meshes: a vertex  $v$  of  $S$ -mesh, together with three of 1-neighborhood adjacent vertices (Figure 12(b)).

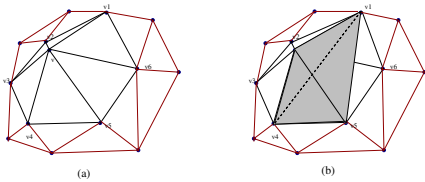


Figure 12: Spatial structure extracted from a 1-neighborhood

Instead of randomly selecting a point in  $S$ -mesh for performing the matching procedure, we use all the vertices whose associated solid angle is above a threshold. In our implementation, it is fixed in  $80^\circ$ . This ensures that no potential matchable pair is missed. For simplicity, we approximate the solid angle of a vertex  $v$  by the median of the angles that all of its incident edges build with its normal vector.

For obtaining the normal vector at  $v$ , we determine the orthogonal regression plane which minimizes the axial distance of the neighboring vertices of  $v$  to it [I.S02]. This regression plane is a good approximation to the tangent plane of the  $S$ -mesh at  $v$ . The vector perpendicular to this plane is, hence, the normal vector of  $S$ -mesh at  $v$ . Let  $v_i, i = 1, \dots, m$ , be the  $m$  vertices of the 1-neighborhood of  $v$ . The covariance matrix  $3 \times 3$  in  $v$  is defined as  $\mathcal{C} = \frac{1}{m} \sum_{i=1}^m (v_i - \bar{v})(v_i - \bar{v})^t$ , where  $\bar{v} = \frac{1}{m} \sum_{i=1}^m v_i$  is the mean position vector. The two eigenvectors, corresponding to the largest eigenvalues, define the regression plane and the third eigenvector is, consequently, its normal vector.

It is worth remarking that, differently from the previous crude registration works, our structure encodes two important intrinsic geometric properties of the vertex  $v$ :

area, approximated by the distances between the adjacent vertices, and curvature, approximated by the angle between the normal vector and the adjacent edges. Hence, we believe that our structure is much more discriminant, in the sense that the number of possible pairings is smaller, without degrading the matching quality.

#### 4.2 Pairwise Local Matching

After the simplification procedure, the number of remaining vertices in  $D$ -mesh is small enough that we can exhaustively look for all possible pairings. It is worth remarking that the QSLIM simplification procedure ensures that regions of similar geometric characteristics are similarly contracted, but does not ensure that connectivity of the edges in these regions is the same. To circumvent this problem, we consider for each vertex  $v$  in  $D$ -mesh all the sample points in  $D$ -image that lie in its 4-neighborhood, when we attempt to find the same tetrahedral structure of  $S$ -mesh in the  $D$ -image (Figure 13). Our search procedure follows the same search space reducing principle of the RBD procedure described in section 1.

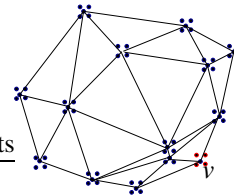


Figure 13: Matchable sample points in  $D$ -image.

Let  $s_i, i = 1..4$  be the vertices of a tetrahedral structure of  $S$ -mesh and let  $d_{ij}$  be the distance between the vertex  $s_i$  and vertex  $s_j$ . The corresponding sample point  $m_1$  of  $s_1$  must be in the 4-neighborhood of the  $s'_1$ 's correspondence in  $D$ -image. The correspondences  $m_2$  and  $m_3$  to  $s_2$  and  $s_3$ , respectively, are obtained in the same way as in the RBD algorithm. And the  $m_4$ , that corresponds to  $s_4$ , must be the intersection of three spheres: the first centered in  $m_1$  and with radius  $d_{14}$ , the second with center in  $m_2$  and radius  $d_{24}$  and the later, centered in  $m_3$  and with radius  $d_{34}$ . Figure 14 illustrates the search spaces for the four correspondences in  $D$ -image.

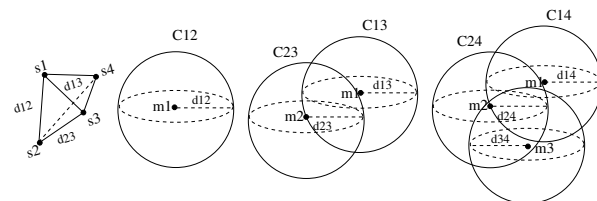


Figure 14: Pairwise matching.

If the correspondences of  $s_i$  are found, we further compare their solid angles. If they are approximately the same, then we consider that  $(s_1, s_2, s_3, s_4)$  and  $(m_1, m_2, m_3, m_4)$  are paired off.

Images	Planar Struct.	Spatial Struct.	% Reduction
Figure 1	11,182,373	1,927,148	82.77%
Figure 2	51,661,440	8,739,339	83.08%
Figure 15	35,402,841	3,242,086	90.84%
Figure 5	125,661,822	3,303,893	97.37%
Figure 6	15,237,324	289,286	98.10%
Figure 7	12,190,662	1,157,796	90.50%
Figure 8	9,253,616	1,391,281	84.97%
Figure 9	24,001,344	909,067	96.21%

Table 1: Planar  $\times$  spatial efficiency comparison

Images	Local Pairings	% Filtering	Iterations ICP
Figure 1	1,927,148	92.38%	6
Figure 2	8,739,339	84.42%	7
Figure 15	3,242,086	73.29%	8
Figure 5	3,303,893	83.32%	7
Figure 6	289,286	89.41%	5
Figure 7	1,157,796	92.72%	4
Figure 8	1,391,281	93.08%	5
Figure 9	909,067	94.00%	8

Table 2: Similarity and visibility efficiency.

To support our remark in Section 4.1, we compared experimentally the filtering efficiency of a planar structure used in the RBD procedure [CHC99] and our proposed spatial structure. Table 1 summarizes in the column 2 and 3, respectively, the number of matchable samples for planar and spatial structures. Observe that the spatial one presents higher filtering efficiency in all of cases.

### 4.3 Additional Filterings

Before estimating the transformation  $T$  that aligns all the range data, we may still filter out some wrong local correspondences that we obtained from the structure matching. There are two trivial tests: neighborhood similarity and visibility tests. In the former, we determine the distance of the aligned points in the vicinity of a matched pair. If it is greater than a pre-specified tolerance, we may discard the correspondence. The latter is based on the fact that if one triangle is on overlapping region, it is visible from the  $S$ -viewpoint, then after alignment it must also be visible from the  $D$ -viewpoint. We apply the visibility test to all 1-neighborhood faces of the locally pairing vertices. If less than 50% of faces pass the test, the correspondence is discarded. Table 2 shows the percentage of the number of matchable points that is reduced after the trivial filtering for the pairs of images presented in this paper. The column Local Pairings provides the number of matchable tetrahedral structures before filtering and the column % Filtering shows the reduction ratio, after filtering, which is in average 87.82%.

## 5 EXPERIMENTAL RESULTS

In this section we present some results that corroborate our conjecture: faithful approximations to dense range images may be used for finding a good correspondence estimate for two partially overlapping range data sets. We apply our algorithm on the data that are similar to the ones employed by Planitz et al. for analyzing and comparing the most known surface correspondence algorithms, namely the spin-image (SIM), the geometric histogram (GHM), the RANSAC-based DARCES (RBD), and the intrinsic curve (ICM) matching procedures. These data vary in acquisition, size, level of detail, and geometric characteristics [BMW05a].

The ANGEL surface pair (Figure 1) and the DINO surface pair (Figure 8) are the same that Planitz et al. used in their work. We also include the FROG surface pair from the Ohio State University repository [OSU] that are  $60^\circ$  apart from each other (Figure 15) and the DRAGON surface pair (Figure 2), scanned with a laser triangulation Cyberware 3030 MS scanner [Sta] and of high level of details.



Figure 15: Range images of a frog.

The rest of surface pairs have been obtained from the Stuttgart repository [Stt]. The CLUB surface pair (Figure 6) was also captured by a Cyberware scanner. It has abrupt curvature variations concentrated in a very small region. The BANANA surface pair (Figure 7) and the MACHINE image pair (Figure 9) are synthetic images from the 3D Cafe website [3dc]. The BANANA images also contain very smooth curvature variations, while the MACHINE surface has sharp edges and planar facets.

Firstly, we apply the QSLIM simplification algorithm in the original data samples, whose number is given in the column Samples of Table 3. The number of vertices of the outcomes are listed in the column Vertices. From these outcomes, our proposed algorithm only selects a few number of tetrahedral structures, as shows the column Structures. The reduction ratio is more than 99.5%. Despite this drastic reduction, our algorithm is able to deliver alignment matrices for the seven surface pairs that make the ICP algorithm converges. Figure 16(a) presents the simplified meshes output by the QSLIM algorithm and Figure 16(b), the visual results of our proposed procedure. These results show that satisfactory crude registration between all the surface pairs is achieved.

According to Planitz et al., we may evaluate quantitatively the performance of our proposal by verifying

Images	Samples	Vertices	Structures
angel <sub>1</sub>	14812	416	54
angel <sub>2</sub>	10632	402	83
bluedino <sub>1</sub>	20494	422	33
bluedino <sub>2</sub>	16783	435	24
frog <sub>1</sub>	9640	297	90
frog <sub>2</sub>	8618	374	56
hub <sub>1</sub>	72099	1039	58
hub <sub>2</sub>	71772	1039	60
banana <sub>1</sub>	21312	542	26
banana <sub>2</sub>	22071	521	24
club <sub>1</sub>	31954	516	22
club <sub>2</sub>	32746	514	25
machine <sub>1</sub>	28086	437	110
machine <sub>2</sub>	33884	552	86
dragon <sub>1</sub>	41841	685	44
dragon <sub>2</sub>	34836	821	80

Table 3: Reduction of samples.

whether its outcomes lead to correct convergence of the ICP procedure. We used the Scanalyze system, developed in the Stanford University [Sca], for evaluating our results. Visually, the outcomes from the Scanalyze is almost indistinguishable from the images shown in Figure 16(b). The column Iterations ICP of Table 2 provides the number of iterations that the ICP algorithm needed to converge to the optimal solution.

## 6 CONCLUDING REMARKS

In this paper we present a technique for an automatic registration of two partially overlapping range images on the basis of their simplified triangular meshes. The most important contribution of our work for crude registrations is to use a faithful approximation of the dense range data. Among the advantages of this approach, we may list: (1) drastic reduction of the input data, without missing the relevant features, (2) easiness in constructing discriminant structures that integrate two intrinsic properties: distance and curvature, and (3) simplicity in defining additional trivial discard rules for pruning false transformations. As further work, we would like to evaluate the sensitive of our method with regard to the threshold of the solid angle and to reconstruct a complete 3D model from the registered range data.

## 7 ACKNOWLEDGMENTS

We would like to acknowledge FAPESP for financial support under the grant numbers 00/10913-3 and 2003/13090-6.

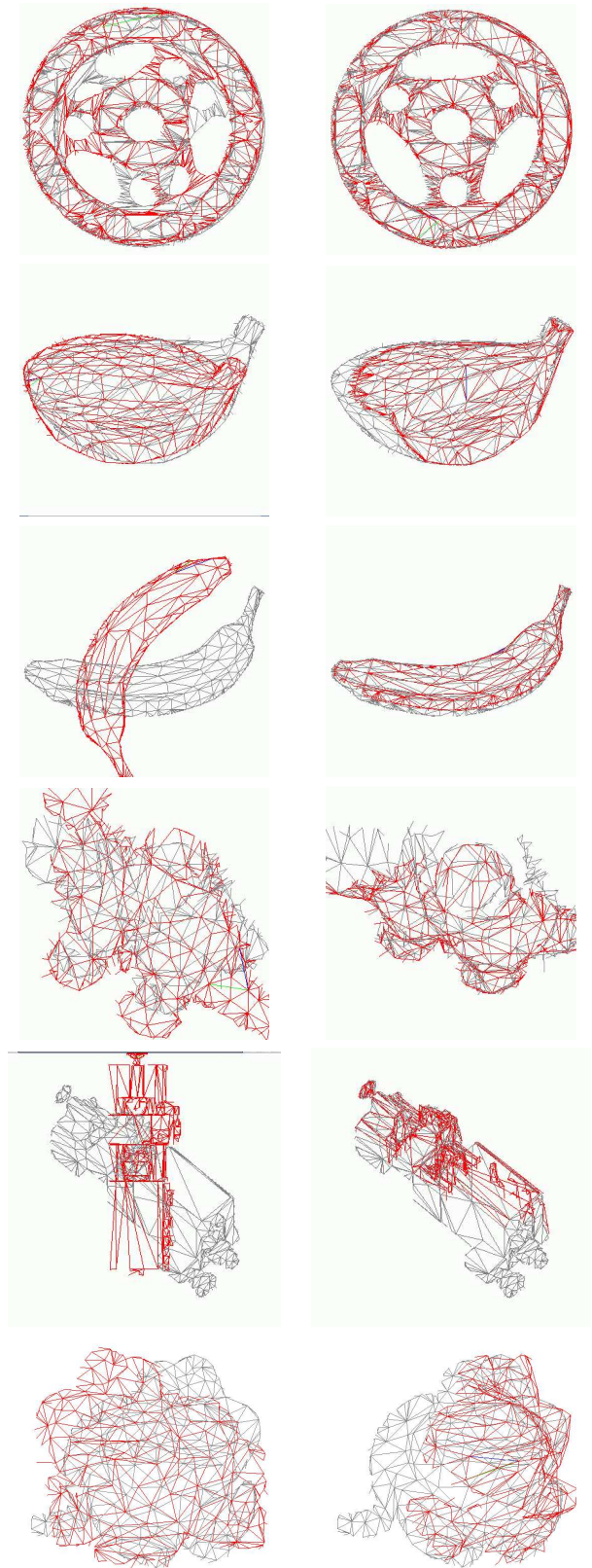
## REFERENCES

[3dc] Range images. <http://www.3dcafe.com/>.

- [AFWR98] A.P. Ashbrook, R.B. Fisher, N. Werghi, and C. Robertson. Aligning arbitrary surfaces using pairwise geometric histograms. In *Proceedings of Noblesse Workshop on Non-linear Model Based Image Analysis*, pages 103–108, 1998.
- [AM99] A.Johnson and M.Hebert. Using spin images for efficient object recognition in cluttered 3d scenes. *IEEE Transactions on Pattern Analysis and Machine Intelligence*, 21:433–448, 1999.
- [BM92] P.J. Besl and N.D. McKay. A method for registration of 3-D shapes. *IEEE Transaction on Pattern Analysis and Machine Intelligence*, 14(2):239–256, 1992.
- [BMW05a] B.M.Planitz, A.J. Maeder, and J.A. Williams. The correspondence framework for 3d surface matching algorithms. *Computer Vision and Image Understanding*, 97:347–383, 2005.
- [BMW05b] B.M.Planitz, A.J. Maeder, and J.A. Williams. Using the correspondence framework to select surface matching algorithms. In *Proceedings of the Australian Pattern Recognition Society (APRS) Workshop on Digital Image Computing*, pages 85–90, 2005.
- [CHC99] Chu-Song Chen, Yi-Ping Hung, and Jen-Bo Cheng. RANSAC-based DARCES: A new approach to fast automatic registration of partially overlapping range images. *IEEE Transactions on Pattern Analysis and Machine Intelligence*, pages 1229–1234, 1999.
- [CM92] Y. Chen and G. Medioni. Object modeling by registration of multiple range images. *Image and Vision Computing*, pages 145–155, 1992.
- [CR02] C.Robertson and R.B.Fisher. Parallel evolutionary registration of range data. *Computer Vision and Image Understanding*, 87:39–50, 2002.
- [GP97] M. Garland and P.Heckbert. Simplification using quadric error metrics. In *Computer Graphics*, volume 31, pages 209–216, New York, USA, 1997.
- [Hor87] B.K.P. Horn. Closed-form solution of absolute orientation using unit quaternions. *Journal of the Optical Society A*, 4(4):629–642, 1987.
- [I.S02] L. I.Smith. A tutorial on principal components analysis. <http://www.cs.otago.ac.nz/COSC453/student-tutorials/>

principal\_components.pdf ,  
Feb. 2002.

- [KA96] K.Brunnstrom and A.J.Stoddart. Genetic algorithms for free-form surface matching. In *Proceedings of 13th International Conference on Pattern Recognition*, volume 4, pages 689–693, 1996.
- [KPH02] Pavel Krsek, Tomáš Pajdla, and Václav Hlaváč. Differential invariants as the base of triangulated surface registration. *Computer Vision Image Understanding*, 87:27–38, 2002.
- [LK05] O.R.P.Bellon L.Silva and K.L.Boyer. Precision range image registration using a robust surface interpenetration measure and enhanced genetic algorithms. *IEEE Transactions on Pattern and Machine Intelligence*, 27:762–776, 2005.
- [MR81] M.A.Fischler and R.C.Bolles. Random sample consensus: A paradigm for model fitting with applications to image analysis and automated cartography. *Comm. Association for Computing Machinery*, 24(6):381–395, 1981.
- [OSU] Range images. <http://sampl.eng.chico-state.edu/sampl/data/3DB/RID> .
- [RL01] S. Rusinkiewicz and M. Levoy. Efficient variants of the ICP algorithm. In *Third International Conf. on 3D Digital Imag. and Modeling*, pages 145–152, 2001.
- [RP96] J-M. Renders and Stéphane P.Flasse. Hybrid methods using genetic algorithms for global optimization. *IEEE Transactions on Systems, Man. and Cybernetics*, 26:243–258, 1996.
- [Sca] Scanalyze, a system for aligning and merging range data. <http://graphics.stanford.edu/software/scanalyze> .
- [Sta] Range images. <http://graphics.stanford.edu/data/3Dscanrep> .
- [Stt] Range images. <http://range.informatik.uni-stuttgart.de/htobcs/html> .
- [WG02] Joris Vanden Wyngaerd and Luc Van Gool. Automatic crude patch registration: Toward automatic 3d model building. *Computer Vision and Image Understanding*, 87(1–3):8–26, July 2002.



(a) Simplified mesh (b) Coarse registration

Figure 16: Crude registration results